

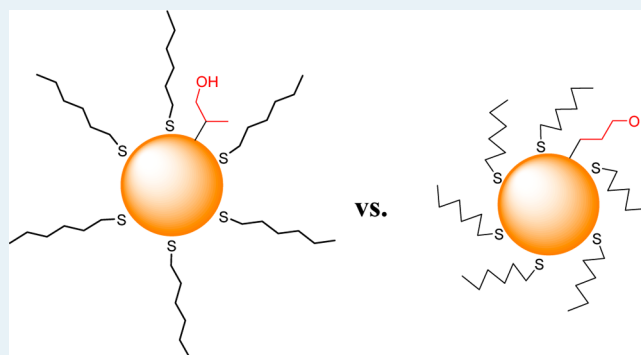
Pd Nanoparticle-Catalyzed Isomerization vs Hydrogenation of Allyl Alcohol: Solvent-Dependent Regioselectivity

Elham Sadeghmoghaddam, Hanmo Gu, and Young-Seok Shon*

Department of Chemistry and Biochemistry, California State University, Long Beach, 1250 Bellflower Blvd., Long Beach, California 90840, United States

ABSTRACT: Our previous work has shown that alkanethiolate-capped Pd nanoparticles generated from sodium *S*-dodecylthiosulfate are excellent catalysts for selective isomerization of various allyl alcohols to the carbonyl analogues. The present work focuses on understanding the mechanism and the regioselectivity of Pd nanoparticles in different environments. First, the presence of H₂ gas has turned out to be essential for the efficient catalytic isomerization reaction. This suggests that the mechanism likely involves the Pd-alkyl intermediate rather than the $\eta^3 \pi$ -allyl Pd hydride intermediate. Second, the Pd nanoparticles are found to convert allyl alcohol selectively to either propanal or 1-propanol depending on the type of solvent used for the catalytic reactions. The reaction pathway is most likely determined by steric hindrance, which is the result of the interaction between substrate and alkylthiolate ligands on Pd nanoparticles. Presumably, the conformation of alkylthiolate ligands changes upon the type of solvents, resulting in varying degree of available space close to the nanoparticle surface. In general, nonpolar or weakly polar solvents such as benzene and chloroform, respectively, promote the isomerization of allyl alcohol to propanal via the formation of the branched Pd-alkyl intermediate. On the other hand, polar protic solvents such as methanol and water foster the hydrogenation of allyl alcohol to 1-propanol involving the steric induced formation of a linear Pd-alkyl intermediate. Third, the use of sodium *S*-hexylthiosulfate instead of sodium *S*-dodecylthiosulfate for the synthesis of Pd nanoparticles results in nanoparticle catalysts with a lower regioselectivity toward isomerization over hydrogenation. This is due to the higher surface ligand density of hexanethiolate-capped Pd nanoparticles, which negatively impacts the formation of branched Pd-alkyl intermediate. The results clearly indicate that controlling the structure and surface density of alkanethiolate ligands around Pd nanoparticles can provide an opportunity to tune the activity and selectivity of nanoparticle catalysts. Lastly, the high stability of soluble nanocatalysts is demonstrated by recycling dodecanethiolate-capped Pd nanoparticles over 10 times for the isomerization reaction of allyl alcohol.

KEYWORDS: Pd, nanoparticles, catalysis, allyl alcohol, isomerization, hydrogenation



INTRODUCTION

Despite popular research interests in alkanethiolate-capped Pd nanoparticles,^{1–6} these nanoparticles have generally not been recognized as efficient catalytic materials.⁷ To our knowledge, alkanethiolate-capped Pd nanoparticles have been successfully utilized for only a handful of organic reactions such as Suzuki and Suzuki–Miyaura C–C bond coupling reactions.^{8,9} However, the aforementioned C–C coupling reactions are also known to be catalyzed by Pd atoms released from the nanoparticle surface.^{10,11} Therefore, it is possible that alkanethiolate-capped Pd nanoparticles may have served as a precursor of the catalytically active Pd species and not been directly involved in the C–C bond coupling reactions. Catalytic reactions using Pd nanoparticles protected with various ligands such as thiolated β -cyclodextrins,¹² tetraalkylammonium salts,^{13,14} and thioethers¹⁵ have also been reported. Dendrimer or polymer encapsulated Pd nanoparticles represent other main efforts to control the catalytic activity of nanoparticles through different surface modifications.^{16–21} In general, the catalytic

activity of Pd nanoparticles has been found to be very sensitive to the particle size, shape, and ligand structure.^{10,11,19}

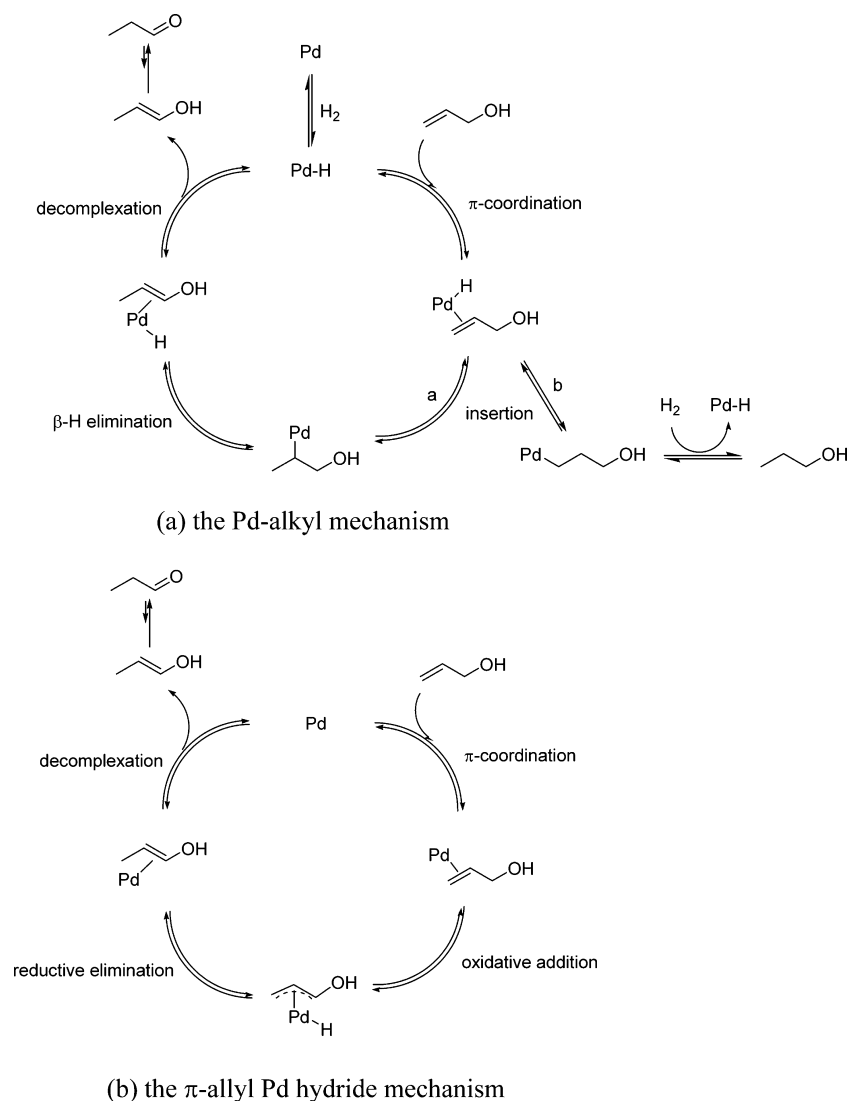
Evaluation of metal catalysts functionalized with well-defined and well-ordered alkanethiolate ligands can be potentially important because such systems can provide a spatial control in the reactivity and selectivity of catalysts. The successful use of alkanethiolate monolayer in controlling activity of supported metal catalysts has been introduced in the recent 2010 report by Marshall et al.²² In addition, controlling the catalytic property of Pd nanoparticles by altering the density of surface alkanethiolate ligands has now been reported from our group.^{23,24} This method utilizes the chemistry of sodium *S*-alkyl thiosulfates, which have previously been used for the generation of thiolate-stabilized gold and silver nanoparticles^{25–28} and self-assembled monolayers on gold and

Received: April 26, 2012

Revised: June 18, 2012

Published: July 18, 2012

Scheme 1. Proposed Mechanisms Accounting for the Isomerization of Allyl Alcohol



copper.^{29–32} The adsorption of thiosulfate is known to produce thiolate monolayers on metal surfaces but is kinetically slower than that of thiols.^{28,29,32} The analysis of produced Pd nanoparticles suggested that the monolayer capped Pd nanoparticles generated from sodium *S*-dodecylthiosulfate have a lower ligand density around Pd nanoparticles because of this difference between thiosulfates and thiols.²³

The previous articles from our group have also shown that the Pd nanoparticles could catalyze selective isomerization over hydrogenation of various allyl alcohols.^{23,24} Catalytically selective transformations of allylic alcohols to either saturated carbonyls via isomerization^{33–36} or saturated alcohols via hydrogenation^{16,19,20} are potentially useful synthetic processes. Although, a number of Pd catalysts have been known for excellent catalytic systems for hydrogenation, the Pd catalysts were usually not able to carry out the isomerization of allyl alcohols with a high selectivity.^{35–37} The catalytic reactions using, for example, heterogeneous Pd/C or Pd-polymer catalysts were unsatisfactory because of the competition between isomerization and hydrogenation processes.^{35–37} One catalytic system based on Pd(OAc)₂ was found to be effective for the isomerization of allyl alcohols, but it required a high temperature (120 °C) for acceptable conversion yields and

was only successful for secondary allyl alcohols.³⁸ The purpose of this research was to understand the mechanism of our Pd nanoparticle catalysts during the isomerization and hydrogenation of allyl alcohol and to examine the regioselectivity of the reactions and the long-term stability of nanocatalysts.

EXPERIMENTAL SECTION

Materials. The following materials were purchased from the indicated suppliers and used as received: Potassium tetrachloropalladate (K₂PdCl₄), tetra-*n*-octylammonium bromide, 1-bromododecane, 1-bromohexane, prop-2-en-1-ol (allyl alcohol), and sodium borohydride (NaBH₄) were purchased from Aldrich. Sodium thiosulfate (Na₂S₂O₃·5H₂O), toluene, acetone, acetonitrile, hexane, methanol, and ethyl alcohol were obtained from Fisher Scientific. Benzene-D₆, chloroform-D, acetone-D₆, methyl alcohol-D₄, deuterium oxide, and dimethyl sulfoxide-D₆ were purchased from Chembridge Isotope. Sodium *S*-dodecylthiosulfate and sodium *S*-hexylthiosulfate were synthesized using a previously published method.²³ Water was purified by a Barnstead NANOpure Diamond ion exchange resins purification unit.

Synthesis of Pd Nanoparticles. The Pd nanoparticle catalysts were synthesized by the following procedure.²⁴ Briefly,

0.13 g (0.4 mmol) of K_2PdCl_4 in 25 mL of water was placed in a reaction flask. The $PdCl_4^{2-}$ was phase-transferred into toluene (50 mL) using 1.09 g (2.0 mmol) of tetraoctylammonium bromide, and the aqueous layer was discarded. A 2-fold molar excess (0.25 g; 0.8 mmol) of sodium S-dodecylthiosulfate in 20 mL (3:1 water/methanol) and 1.09 g (2.0 mmol) of tetraoctylammonium bromide were added to the reaction mixture. The reaction mixture was stirred for about 10 min at room temperature, before adding 0.30 g (8.0 mmol) of $NaBH_4$ in 15 mL of nanopure water over a period of about 10 s. The solution was quickly darkened during borohydride addition. After being stirred for 3 h, the water phase was discarded and the toluene was removed under vacuum, leaving a black solid. The black precipitate was suspended in 50 mL of ethanol and placed on a glass filtration frit. The product was exhaustively washed with ethanol, acetonitrile, and acetone.

Catalytic Reactions. The catalysis experiments were performed by placing 3 mL of fresh solvent ($CDCl_3$, C_6D_6 , etc) in a 250 mL reaction flask. To this was added 18.63 mg (5 mol % based on the mole ratio of Pd to reactant) of palladium nanoparticle catalyst. The catalyst was conditioned under hydrogen gas for 10 min before 0.2 mL (2.9 mmol) of allyl alcohol was injected in to the reaction mixture. The reaction mixture was then stirred under atmospheric pressure and at room temperature. The catalytic reaction was allowed to continue for a predetermined time, in which a NMR of the solution was obtained. When polar solvents (acetone, dimethyl sulfoxide, methanol, and water) were used as reaction medium, the nanoparticles were stirred while suspended in solution. The insoluble aggregates of nanoparticles generated in these solvents act as heterogeneous catalysts.

Measurements. Proton NMR spectra were recorded on a Bruker AC400 FT-NMR spectrometer operating at 400 MHz in $CDCl_3$ solutions and internally referenced to δ 7.26 ppm. UV-vis spectra of nanoparticle solutions in quartz cells were acquired on a UV-2450 Shimadzu UV-vis spectrophotometer. Transmission electron microscopy (TEM) images of nanoparticles were obtained with a JEOL 1200 EX II electron microscope operating at 100 keV. Samples were prepared for TEM by casting a single drop of a ~ 1 mg/mL tetrahydrofuran (THF) solution onto a standard carbon-coated (80–100 Å) Formvar film on copper grids (400 mesh) and drying in air for at least 30 min. Several regions were imaged at $100,000\times$. Size distributions of the Pd cores were obtained from digitized photographic enlargements with Scion Image Beta Release 2. Thermogravimetric analysis (TGA) was conducted on a TA Instruments QDT 600 using an ultrahigh purity (UHP) nitrogen atmosphere (flow rate of 100 mL/min), with heating from room temperature to 600 °C at a heating rate of 20 °C/min.

RESULTS AND DISCUSSION

Over the years, two different mechanisms shown in Scheme 1 have been proposed to explain the Pd-based catalytic isomerization and hydrogenation of allylic alcohols.³⁶ The first mechanism shown in Scheme 1(a) is known as the Pd-alkyl mechanism and requires the presence of the Pd–H species before the adsorption of allyl alcohol and the initiation of catalytic reaction. The addition of H_2 gas or the presence of surface H is, therefore, necessary for this Pd-alkyl mechanism to take place. As shown in Scheme 1(a), the insertion mode of Pd–H to the π bond of allyl alcohol is particularly important and most likely determines the selectivity of reaction. Because

Table 1. Isomerization vs Hydrogenation of Allyl Alcohol in Different Gas Environments^a

gas	conversion (%)	catalysis results (%) (hydrogenation: isomerization)		reaction time (hours)
12 mmol H_2	100	5	95	4
12 mmol H_2 + N_2 flush	0	0	0	4
continuous H_2 flow	85	35	50	4
air	5	2	3	48

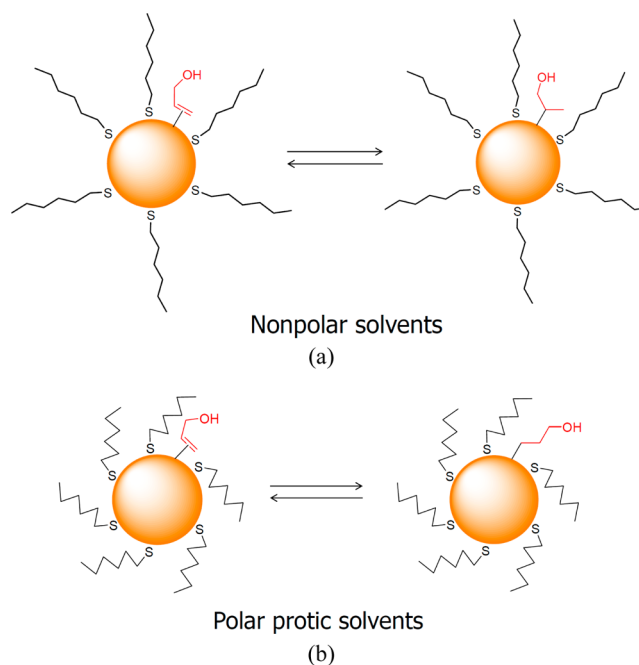
^a25 °C in $CHCl_3$.

Table 2. Isomerization vs Hydrogenation in Different Solvents at 25 °C

solvents	conversion (%)	catalysis results (ratio) (hydrogenation: isomerization)		reaction time (hours)
C_6H_6	64	0	100	24
$CHCl_3$	100	5	95	24 ^b
Acetone ^a	46	30	70	24
DMSO ^a	39	21	79	24
CH_3OH ^a	47	100	0	24
H_2O ^a	65	74	26	24

^aPd nanoparticles are insoluble in the indicated solvents making the catalytic reactions heterogeneous. ^bThe reaction completes in 4 h based on the kinetic studies.²⁴

Scheme 2. Proposed Mechanisms Accounting for the Isomerization and Hydrogenation of Allyl Alcohol in Different Solvents



the carbonyl products are generated from the tautomerization of enol intermediate, the insertion of Pd–H to $C=C$ should follow a Markovnikov addition pattern and produce a branched Pd-alkyl intermediate (route a). In comparison, the anti-Markovnikov addition of Pd–H to the π -bond produces a linear Pd-alkyl intermediate and increases the hydrogenation of

Table 3. Isomerization vs Hydrogenation in Different Solvents at 70 °C^a

solvents	conversion (%)	catalysis results (ratio)		reaction time (hours)
		(hydrogenation: isomerization)	(hydrogenation: isomerization)	
C ₆ H ₆	100	2	98	6, 24
DMSO ^b	78	10	90	6
	100	17	83	24
CH ₃ OH ^b	83	100	0	24
H ₂ O ^b	100	71	29	24

^aAt 70 °C, the nanoparticles were stable up to 24 h. However, the continuous heating over more than one day at the same temperature started to cause some aggregation and precipitation of nanoparticles.

^bPd nanoparticles are insoluble in the indicated solvents making the catalytic reactions heterogeneous.

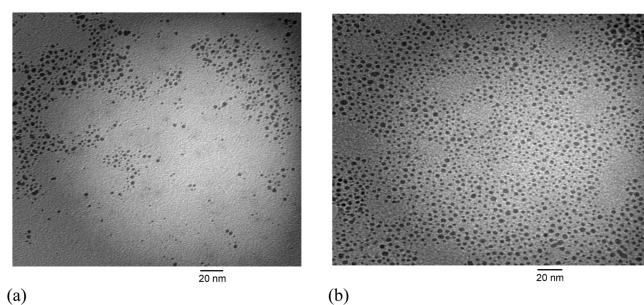


Figure 1. TEM images of (a) hexanethiolate (C6S)- and (b) dodecanethiolate (C12S)-capped Pd nanoparticles generated from the corresponding Bunte salts.

allyl alcohol (route b). A major difference of the π -allyl Pd hydride mechanism shown in Scheme 1(b) is that the reaction does not require the presence of H₂ gas, because the Pd–H adduct is generated from the oxidative addition of Pd to the C–H bond α to the OH group. The entire reaction in Scheme 1(b) is also an intramolecular reaction.

To understand the mechanism of catalytic reactions involving our alkanethiolate-capped Pd nanoparticles, the homogeneous catalytic reactions of allyl alcohol using dodecanethiolate (C12S)-capped Pd nanoparticles were studied in different gas environments (Table 1). The results showed that the catalytic reaction with 12 mmol H₂ gas capped in the reaction flask for 4 h led to a complete conversion of allyl alcohol with a very high selectivity (95%) for isomerization reaction. Flushing H₂ gas with N₂ gas resulted in a complete loss of catalytic activity of Pd nanoparticles. With the absence of any significant amount of H₂ gas (in the case of catalytic reaction in air), the reaction also resulted in a negligible catalytic conversion of allyl alcohol even after the extended reaction time (48 h). This result supported that the presence of H₂ gas was essential for the catalytic conversion of allyl alcohol using C12S-capped Pd nanoparticles. The presence of excess H₂ gas with the continuous H₂ gas flow

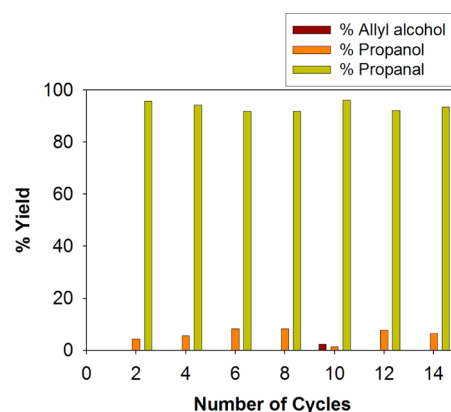


Figure 2. Recycling profiles of the catalytic isomerization of allyl alcohol using dodecanethiolate-capped Pd nanoparticles.

made the reaction less selective, producing an increased amount of hydrogenation product. In addition, the continued flow of H₂ gas into the reaction flask slowed the reaction down noticeably. This was likely due to a decrease in actual binding sites for allyl alcohol resulted from the presence of excess surface-bound H on the nanoparticle surface. The results clearly suggested that the presence of H₂ gas was a requirement for the catalytic reaction of allyl alcohol and proved that the mechanism of this reaction is most likely the Pd-alkyl mechanism instead of the π -allyl Pd hydride mechanism. Further results supporting the Pd-alkyl intermediate as its main reaction mechanism are presented in the later part of this article.

The catalytic reaction of allyl alcohol was also studied in various solvents to understand the role of the thiolate ligands surrounding Pd nanoparticles in different chemical environments. Six different solvents representing nonpolar, polar aprotic, and polar protic solvents were chosen for the investigation. Pd nanoparticles are only soluble in nonpolar solvents such as C₆H₆ and CHCl₃, because the particles are capped with nonpolar alkanethiolate ligands. Since acetone and dimethylsulfoxide (DMSO) are polar aprotic solvents, the difference in the polarity of ligands and solvents makes Pd nanoparticles insoluble and aggregated. The Pd nanoparticles in two polar protic solvents (H₂O and CH₃OH) are also aggregated.

First, the soluble Pd nanoparticles in two nonpolar solvents (C₆H₆ and CHCl₃) were compared and the results are shown in Table 2. In CHCl₃, the catalytic reaction was completed in 4 h and resulted in 95% propanal along with 5% propanol. The possible further hydrogenation of produced propanol to 1-propanol was examined, and the results confirmed the inactivity of Pd nanoparticles generated from *S*-dodecylthiosulfate for the catalytic hydrogenation of carbonyl compounds. When the reaction was performed in C₆H₆, only a single product in the form of propanal was produced, indicating a higher selectivity

Table 4. TEM and TGA Results and Allyl Alcohol Catalysis Results of Hexanethiolate (C6S)- and Dodecanethiolate (C12S)-Capped Pd Nanoparticles

nanoparticle	TEM (nm)	TGA (organic %)	conversion (%)	catalysis results (%)		reaction time (hours)
				hydrogenation	isomerization	
C6S	2.6 ± 1.3	20.2	42	11	31	4
			100	13	87	24
C12S	2.6 ± 1.1	25.0	100	5	95	4

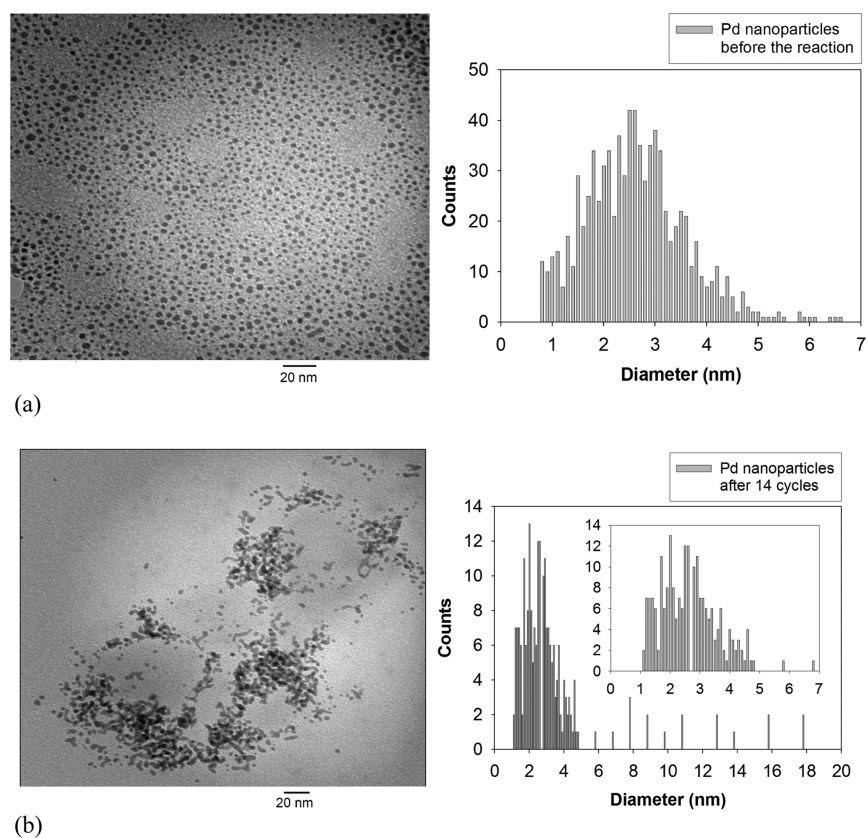


Figure 3. TEM images and histograms of dodecanethiolate (C12S)-capped Pd nanoparticles (a) before and (b) after multiple catalytic reactions.

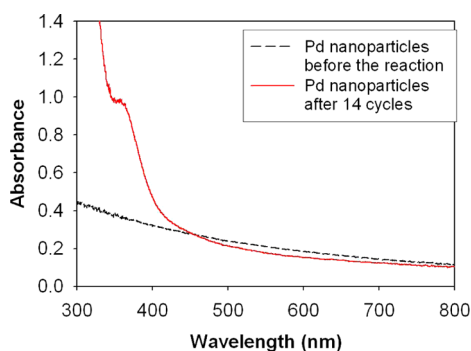


Figure 4. UV-vis spectra of dodecanethiolate (C12S)-capped Pd nanoparticles before and after multiple catalytic reactions.

for isomerization over hydrogenation in C_6H_6 . However, the catalytic isomerization of allyl alcohol was only limited to 64% conversion even after 24 h reaction. It is speculated that the interaction of benzene molecules on the nanoparticle surface likely causes a temporary deactivation of the Pd surfaces and a decrease in the rate of the catalytic reaction.³⁹ Similar kinetic hindrance was also observed from the catalytic reactions of allyl alcohol mixtures and was discussed in the earlier publication.²⁴

Second, the catalytic reactions of allyl alcohol using aggregated Pd nanoparticles were studied in polar aprotic solvents (acetone and DMSO). In general, the heterogeneous reactions are known to be slower than the homogeneous reactions. The same trend could be observed from the catalytic reactions using aggregated Pd nanoparticles in polar aprotic solvents. In this condition, the ligands on aggregated nanoparticles are interdigitated and the density of ligands on the surface is increased. As a result, the ligands on nanoparticles will

not be as open as the ones in the nonpolar solvents, which should cause a decrease in the rate of reactions in polar solvents. The compact structure of surrounding ligands because of hydrophobic-like effects in these solvents and the decreased solvent swelling that should become kinetic barriers for incoming reactants are also contributing factors. In polar aprotic solvents, although the isomerization of allyl alcohol was still more favored over the hydrogenation, the selectivity toward isomerization was somewhat decreased. Looking back at Scheme 1(a), which is the most probable reaction mechanism for the isomerization of allyl alcohol using Pd nanoparticles, it is clear that the regioselective formation of Pd-alkyl intermediate (Markovnikov vs anti-Markovnikov addition of Pd-H to C=C; route a vs route b, respectively) is important and should have a dramatic effect on the results of catalysis reactions. Considering both the reaction mechanism in Scheme 1(a) and the structure of alkanethiolate ligands in different solvents, the formation of two different Pd-alkyl intermediates generated from the regioselective addition of Pd-H to C=C on particle surfaces are proposed (Scheme 2). In these mechanisms, the regioselective reaction pathways are most likely determined by steric hindrance, which is the result of the interaction between substrate and alkanethiolate ligands on Pd nanoparticles. Presumably, the conformation of alkanethiolate ligands changes upon the type of solvents, resulting in varying degree of available space near the nanoparticle surfaces. Attributable to the steric hindrance created by contracted ligands, the formation of branched Pd-alkyl intermediate becomes a little less favorable in polar aprotic solvents compared to in nonpolar solvents.

Third, the catalytic reactions of allyl alcohol in polar protic solvents (methanol and water) were also turned out to be

slower than the reactions in nonpolar solvents. However, the catalytic reactions in these solvents resulted in a higher selectivity for hydrogenation, producing 1-propanol as a major product, instead of isomerization. Especially in methanol, the hydrogenation of allyl alcohol took place without the isomerization to propanal, which was completely opposite from the results observed from the catalytic reactions in nonpolar solvents. The large difference in the selectivity of reactions in nonpolar and polar protic solvents suggested the favorable formation of different intermediates during the catalytic reactions in these solvents. Owing to strong hydrophobic effects in these solvents, the alkanethiolate ligands surrounding Pd nanoparticles will be highly contracted. Therefore, in polar protic solvents, the decreased space resulted from the particle aggregation and the hydrophobic effects likely promotes the anti-Markovnikov addition of Pd–H and the formation of the linear Pd-alkyl intermediate (Scheme 2(b)) rather than the branched Pd-alkyl intermediate shown in Scheme 2(a).

Despite the fact that the data is consistent with the interpretation based on this steric crowding of the Pd surface with the different ligands and in the different solvents, the possibility of other factors besides the steric hindrance affecting the selectivity of catalytic reactions cannot be completely ruled out. One of other possibilities for the increased selectivity toward the hydrogenation would be the participation of methanol and water, which have an ability to provide extra surface H on to Pd surfaces, during the reactions. However, the catalytic reactions performed in methanol-D₄ and D₂O did not indicate any incorporation of deuterium to 1-propanol in the NMR spectra. This result indicated that the mechanism does not involve the formation of Pd–D adduct during the catalytic reactions in methanol and water. More systematic and mechanistic investigations will look into the possibility of other important factors in determining the selectivity of nanocatalysts in the near future.

The catalytic reactions in different solvents were also performed at higher temperature to see if the regioselectivity of reactions changes upon the increase in the reaction temperature. As shown in Table 3, the increasing temperature of catalytic reactions improved the overall conversion of allyl alcohol in both polar (DMSO, methanol, and water) and nonpolar solvent (benzene) systems. The catalytic reaction in C₆H₆ at 70 °C resulted in a complete conversion of allyl alcohol in 6 h and produced the isomerization product (propanal) in 98% yield, suggesting a high regioselectivity of the reaction. In polar aprotic solvent (DMSO), the reaction required 24 h for the complete conversion of allyl alcohol and produced a higher percentage of the isomerization product than the hydrogenation product, maintaining the same regioselectivity trend observed from the catalytic reactions at lower temperature. The overall conversion of allyl alcohol in polar protic solvents also improved for the catalytic reactions at higher temperature. The regioselectivity trend also remained same, having 1-propanol as a major product in both methanol and water. The hydrogenation product (1-propanol) was again the only product produced in methanol after 24 h reaction. Overall, the higher temperature clearly improved the yield of the reactions and still maintained the same regioselectivity. The conformation of alkanethiolate ligands and the resulting available space on the Pd nanoparticle surface in different solvents still remain important at higher reaction temperature and control the regioselectivity of the catalytic reactions.

The effects of alkanethiolate ligand chain length on the synthesis and the catalytic property of Pd nanoparticles were also investigated. TEM results suggested that both Pd nanoparticles with dodecanethiolate (C12S) and hexanethiolate (C6S) ligands have similar average core dimensions (Figure 1). However, the organic weight fraction of C6S-capped Pd nanoparticles derived from TGA results was only slightly lower than that of C12S-capped Pd nanoparticles. When the molecular weights of two ligands were taken into account, this result indicated that Pd nanoparticles with different average ligand packing density have been produced despite the particles being synthesized under the same condition. The combination of TEM and TGA results confirmed that Pd nanoparticles generated from sodium S-hexylthiosulfate were capped with a higher density of hexanethiolate ligands (average molecular formula: Pd₄₅₉(SC6)₁₀₄ compared to Pd₄₅₉(SC12)₈₁).⁴⁰ This is likely due to the smaller size of the S-hexylthiosulfate and the use of nonpolar toluene solvent as a reaction medium for the nanoparticle synthesis that can induce more facile adsorption of S-hexylthiosulfate on to the surface of Pd nanoparticles. The relatively high polarity of S-hexylthiosulfate should cause less solvation in nonpolar solvent. Therefore, the adsorption of S-hexylthiosulfate can be kinetically faster than that of S-dodecylthiosulfate in toluene. Similar kinetic phenomena have been frequently observed from the self-assembly of ω -functionalized alkanethiols on flat metal substrates and metal nanoparticle surfaces.^{41,42} However, the average core size of nanoparticles was not affected by these differences in S-alkylthiosulfate ligands, which was likely due to the presence of excess surfactant, tetraoctylammonium bromide. This result suggested that it might be possible for us to further control the density of alkanethiolate ligands on Pd nanoparticles more precisely using the thiosulfate synthetic protocol. The possibility of controlling the catalytic property and the composition of alkanethiolate-capped metal nanoparticles is currently being investigated in our lab by the careful modification of various synthetic conditions.

The catalytic activity of Pd nanoparticles with a higher density of C6S ligands and a lower density of C12S ligands are compared and the results are shown in Table 4. Because of the higher average density of surface ligands, the catalytic activity of C6S-capped Pd nanoparticles was slightly lower than that of C12S-capped Pd nanoparticles requiring an extended reaction time (24 h) for a complete reaction. The favorable trends for isomerization remained same, but the higher density of C6S ligands around Pd nanoparticles slightly lowered the regioselectivity of catalytic reactions, which produced the increased amount of hydrogenation products. This result also supports our previous conclusion that the regioselectivity of catalytic reactions depends on the steric hindrance created by the interaction between the substrate (allyl alcohol) and the alkanethiolate ligands on Pd nanoparticles and the resulting structure of Pd-alkyl intermediates.

Catalyst recycling is attempted to investigate the efficiency of Pd nanoparticle catalyst systems. Ligand-capped metal nanoparticles have been recognized as a good candidate for semiheterogeneous catalysts because they can be easily separated from the reaction mixture in homogeneous condition.¹⁰ The alkanethiolate-capped Pd nanoparticles could be precipitated from the homogeneous solution by the addition of polar solvents such as methanol and the subsequent isolation from the reaction mixture by centrifugation and decantation of reaction products and solvents. The long-term

stability of Pd nanoparticles was also tested by a repeated usage of recycled catalysts for the reaction of allyl alcohol. Figure 2 shows the yields of propanal and 1-propanol over the period of 14 cycles. The results clearly showed that the recycled Pd nanoparticle catalysts maintained a high activity after repeated precipitation and redissolution in the reaction medium. To examine the possibility of nanoparticle morphological changes after the repeated catalyst recycling, the Pd nanoparticles were characterized by TEM (Figure 3) and UV-vis spectroscopy (Figure 4). TEM results and the histogram analysis (Figure 3) showed the high population of small Pd nanoparticles even after the multiple recycling. Although some particles clearly underwent morphological changes from spherical to elongated rod shape, the high activity of nanoparticle catalysts after the multiple cycles suggested that the small Pd nanoparticles in large quantities are the main active catalysts for the isomerization of allyl alcohol. Interestingly, the UV-vis results of recycled Pd nanoparticles showed the absorption band at ~360 nm, which corresponds to the Pd(II) species. This suggested that Pd-thiolate species might be generated during the catalytic reactions after multiple recycling. Since it has been found that Pd(II)-alkanethiolates are poor catalysts for the isomerization and hydrogenation of allyl alcohol,²³ the participation of desorbed Pd(II)-alkanethiolates from nanoparticle surfaces for the catalysis of allyl alcohol should be negligible.

CONCLUSION

Pd nanoparticles prepared from S-dodecylthiosulfate could be used for both catalytic isomerization and hydrogenation of allyl alcohol depending on the type of solvent used during the reaction. The mechanism of the reaction involves the Pd-alkyl intermediate, and the regioselectivity of reaction is controlled by the step involving either Markovnikov or anti-Markovnikov addition pathways. In general, nonpolar solvents promote the isomerization of allyl alcohol to propanal, and polar protic solvents foster the hydrogenation of allyl alcohol to 1-propanol. The presence of shorter alkylthiolate ligands on Pd nanoparticles results in a lower regioselectivity for the isomerization reaction. This is due to the higher surface ligand density of hexanethiolate-capped Pd nanoparticles compared to that of dodecanethiolate-capped Pd nanoparticles synthesized under the same synthetic condition. The results clearly indicated that controlling the structure and conformation of alkanethiolate ligands on Pd nanoparticles might bring about the development of highly selective and efficient catalytic materials. Lastly, the high stability of soluble nanocatalysts is demonstrated by recycling dodecanethiolate-capped Pd nanoparticles 14 times for the isomerization reaction.

AUTHOR INFORMATION

Corresponding Author

*E-mail: ys.shon@csulb.edu. Phone: 562-985-4466. Fax: 562-985-8547.

Funding

This research was supported in part by a grant from the ACS-PRF (PRF49407-UR7) and CSULB (MGSS award).

Notes

The authors declare no competing financial interest.

REFERENCES

- (1) Yang, Z.; Klabunde, K. J.; Sorensen, C. M. *J. Phys. Chem. C* **2007**, *111*, 18143–18147.
- (2) Garcia-Martinez, J. C.; Scott, R. W. J.; Crooks, R. M. *J. Am. Chem. Soc.* **2003**, *125*, 11190–11191.
- (3) Zamborini, F. P.; Gross, S. M.; Murray, R. W. *Langmuir* **2001**, *17*, 481–488.
- (4) Chen, S.; Huang, K.; Stearns, J. A. *Chem. Mater.* **2000**, *12*, 540–547.
- (5) Sun, Y.; Frenkel, A. I.; Isseroff, R.; Shonbrun, C.; Forman, M.; Shin, K.; Koga, T.; White, H.; Zhang, L.; Zhu, Y.; Rafailovich, M. H.; Sokolov, J. C. *Langmuir* **2006**, *22*, 807–816.
- (6) Quiros, I.; Yamada, M.; Kubo, K.; Mizutani, J.; Kurihara, M.; Nishihara, H. *Langmuir* **2002**, *18*, 1413–1418.
- (7) Chauhan, B. P. S.; Rathore, J. S.; Bando, T. *J. Am. Chem. Soc.* **2004**, *126*, 8493.
- (8) Cargnello, M.; Wieder, N. L.; Canton, P.; Montini, T.; Giambastiani, G.; Benedetti, A.; Gorte, R. J.; Fornasiero, P. *Chem. Mater.* **2011**, *23*, 3961–3969.
- (9) Lu, F.; Ruiz, J.; Astruc, D. *Tetrahedron Lett.* **2004**, *45*, 9443–9445.
- (10) Astruc, D.; Lu, F.; Aranzaes, J. R. *Angew. Chem., Int. Ed.* **2005**, *44*, 7852–7872.
- (11) Astruc, D. *Inorg. Chem.* **2007**, *46*, 1884–1894.
- (12) Liu, J.; Alvarez, J.; Ong, W.; Román, E.; Kaifer, E. *Langmuir* **2001**, *17*, 6762–6764.
- (13) Reetz, M. T.; de Vries, J. G. *Chem. Commun.* **2004**, 1559.
- (14) Reetz, M. T.; Westermann, E. *Angew. Chem., Int. Ed.* **2000**, *39*, 165–168.
- (15) Ganesan, M.; Freemantle, R. G.; Obare, S. O. *Chem. Mater.* **2007**, *19*, 3464–3471.
- (16) Wilson, O. M.; Knecht, M. R.; Garcia-Martinez, J. C.; Crooks, R. M. *J. Am. Chem. Soc.* **2006**, *128*, 4510–4511.
- (17) Oh, S.-K.; Niu, Y.; Crooks, R. M. *Langmuir* **2005**, *21*, 10209–10213.
- (18) Li, Y.; El-Sayed, M. A. *J. Phys. Chem. B* **2001**, *105*, 8938–8943.
- (19) Bhattacharjee, S.; Dotzauer, D. M.; Bruening, M. L. *J. Am. Chem. Soc.* **2009**, *131*, 3601–3610.
- (20) Kidambi, S.; Dai, J.; Li, J.; Bruening, M. *J. Am. Chem. Soc.* **2004**, *126*, 2658–2659.
- (21) Hu, J.; Liu, Y. *Langmuir* **2005**, *21*, 2121–2123.
- (22) Marshall, S. T.; O'Brien, M.; Oetter, B.; Corpuz, A.; Richards, R. M.; Schwartz, D. K.; Medlin, J. W. *Nat. Mater.* **2010**, *9*, 853–858.
- (23) Sadeghmoghaddam, E.; Lam, C.; Choi, D.; Shon, Y.-S. *J. Mater. Chem.* **2011**, *21*, 307–312.
- (24) Sadeghmoghaddam, E.; Gaieb, K.; Shon, Y.-S. *Appl. Catal., A* **2011**, *405*, 137–141.
- (25) Lohse, S. E.; Dahl, J. A.; Hutchison, J. E. *Langmuir* **2010**, *26*, 7504–7511.
- (26) Mari, A.; Imperatori, P.; Marchegiani, G.; Pilloni, L.; Mezzi, A.; Kaciulis, S.; Cannas, C.; Meneghini, C.; Mobilio, S.; Suber, L. *Langmuir* **2010**, *26*, 15561–15566.
- (27) Shon, Y.-S.; Cutler, E. *Langmuir* **2004**, *20*, 6626–6630.
- (28) Shon, Y.-S.; Gross, S. M.; Dawson, B.; Porter, M.; Murray, R. W. *Langmuir* **2000**, *16*, 6555–6561.
- (29) Fealy, R. J.; Ackerman, S. R.; Ferguson, G. S. *Langmuir* **2011**, *27*, 5371–5376.
- (30) Labukas, J. P.; Drake, T. J. H.; Ferguson, G. S. *Langmuir* **2010**, *26*, 9497–9505.
- (31) Lusk, A. T.; Jennings, G. K. *Langmuir* **2001**, *17*, 7830–7836.
- (32) Lukkari, J.; Meretoja, M.; Kartio, I.; Laajalehto, K.; Rajamäki, M.; Lindström, M.; Kankare, J. *Langmuir* **1999**, *15*, 3529–3537.
- (33) Leung, D. H.; Bergman, R. G.; Raymond, K. N. *J. Am. Chem. Soc.* **2007**, *129*, 2746–2747.
- (34) Cadierno, V.; Garcia-Garrido, S. E.; Gimeno, J.; Varela-Álvarez, A.; Sordo, J. A. *J. Am. Chem. Soc.* **2006**, *128*, 1360–1370.
- (35) Van der Drift, R. C.; Bouwman, E.; Drent, E. *J. Organomet. Chem.* **2002**, *650*, 1–24.
- (36) Uma, R.; Crévisy, C.; Grée, R. *Chem. Rev.* **2003**, *103*, 27–51.
- (37) Zharmagambetova, A. K.; Ergozhin, E. E.; Sheludiyakov, Y. L.; Mukhamedzhanova, S. G.; Kurmanbayeva, I. A.; Selenova, B. A.; Utkelov, B. A. *J. Mol. Catal. A: Chem.* **2001**, *177*, 165–170.

- (38) Ganchegui, B.; Bouquillon, S.; Hénin, F.; Muzart, J. J. *Mol. Catal. A: Chem.* **2004**, *214*, 65–69.
- (39) de M. Cruz, M. T.; de M. Carneiro, J. W.; Aranda, D. A. G.; Bühl, M. J. *Phys. Chem. C* **2007**, *111*, 11068.
- (40) Hostetler, M. J.; Wingate, J. E.; Zhong, C.-J.; Harris, J. E.; Vachet, R. W.; Clark, M. R.; Londono, J. D.; Green, S. J.; Stokes, J. J.; Wignall, G. D.; Glish, G. L.; Porter, M. D.; Evans, N. D.; Murray, R. W. *Langmuir* **1998**, *14*, 17–30.
- (41) Ostuni, E.; Yan, L.; Whitesides, G. M. *Colloids Surf., B* **1999**, *15*, 3.
- (42) Choo, H.; Cutler, E.; Shon, Y.-S. *Langmuir* **2003**, *19*, 8555–8559.